A STING-Activating Nanovaccine for Cancer Immunotherapy

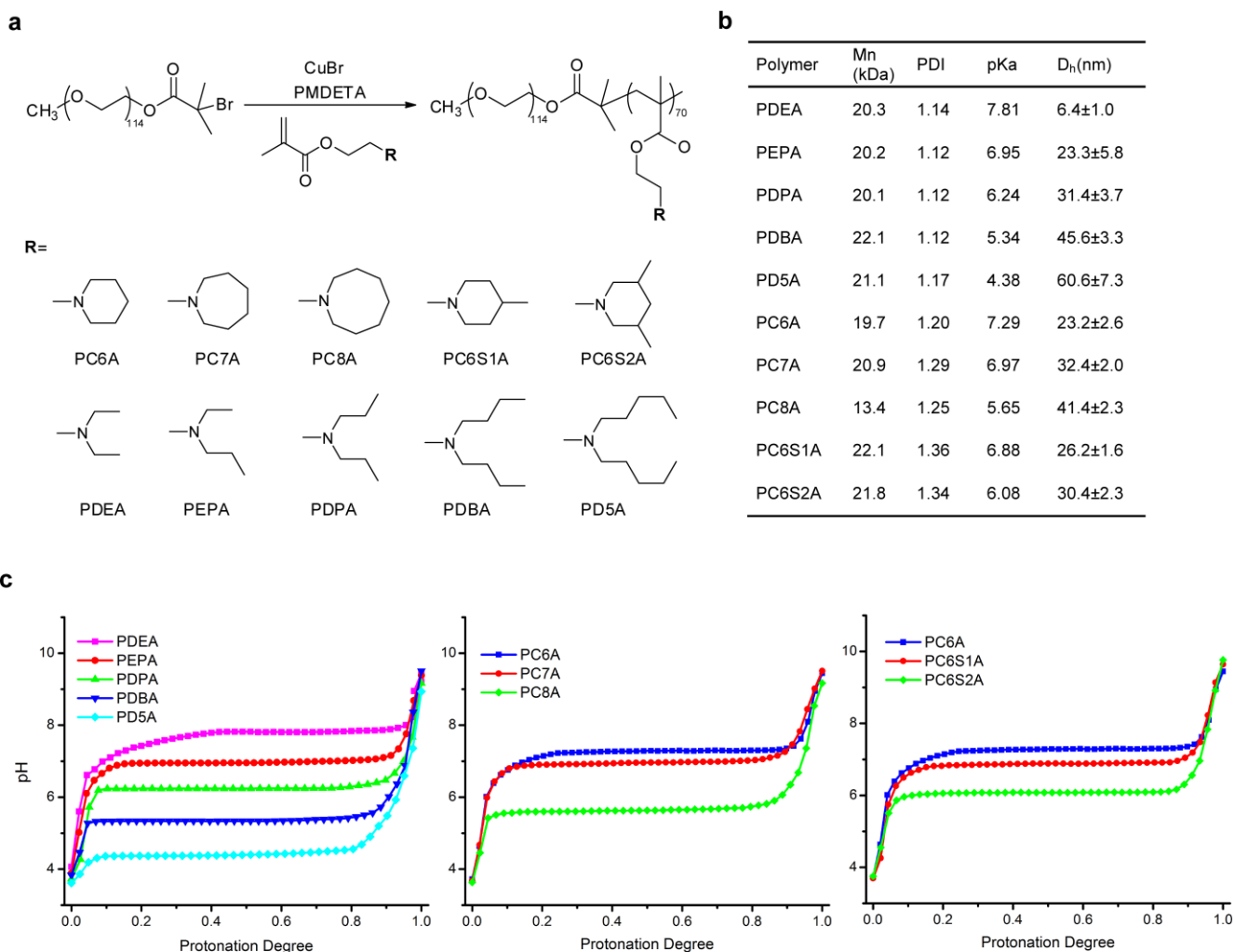Min Luo[1,†], Hua Wang[2,†], Zhaohui Wang[1,†], Haocheng Cai[2], Zhigang Lu[3], Yang Li[1], Mingjian Du[2], Gang Huang[1], Chensu Wang[1], Xiang Chen[2], Matthew R. Porembka[4], Jayanthi Lea[5], Arthur E. Frankel[6], Yang-Xin Fu[7], Zhijian J. Chen[2,8,*] and Jinming Gao[1,*]

[1]*Department of Pharmacology, Simmons Comprehensive Cancer Center;* [2]*Department of Molecular Biology;* [3]*Department of Developmental Biology;* [4]*Department of Surgery;* [5]*Department of Obstetrics and Gynecology;* [6]*Department of Internal Medicine;* [7]*Department of Pathology;* [8]*Howard Hughes Medical Institute, University of Texas Southwestern Medical Center, 5323 Harry Hines Blvd., Dallas, Texas 75390, USA*

[†]These authors contributed equally to this work.

[*]Co-corresponding authors.

Correspondence and requests for materials should be addressed to J.G. (jinming.gao@utsouthwestern.edu) or Z.J.C (zhijian.chen@utsouthwestern.edu).

a

b

Polymer	Mn (kDa)	PDI	pKa	D_h(nm)
PDEA	20.3	1.14	7.81	6.4±1.0
PEPA	20.2	1.12	6.95	23.3±5.8
PDPA	20.1	1.12	6.24	31.4±3.7
PDBA	22.1	1.12	5.34	45.6±3.3
PD5A	21.1	1.17	4.38	60.6±7.3
PC6A	19.7	1.20	7.29	23.2±2.6
PC7A	20.9	1.29	6.97	32.4±2.0
PC8A	13.4	1.25	5.65	41.4±2.3
PC6S1A	22.1	1.36	6.88	26.2±1.6
PC6S2A	21.8	1.34	6.08	30.4±2.3

c

Supplementary Figure 1

**Syntheses and pH titration of ultra-pH sensitive (UPS) PEG-*b*-PR block copolymers.**

(**a**) Schematic syntheses of block copolymers using an atom-transfer radical polymerization (ATRP) method. PEG-Br (MW = 5 kD) was used as an initiator and metharylates with different tertiary amine side chains were used as monomers. (**b**) Characterization of the copolymers from the library. Number-averaged molecular weight (Mn) was determined by GPC using THF as the eluent; pKa was determined by pH titration of polymer solutions using 4 M NaOH. Size was measured using dynamic light scattering, mean ± s.d. (**c**) pH titration of UPS copolymers displayed pH-specific buffer effect from pH 4 to 8. For the cyclic series, both the size of cyclic rings (i.e., 6, 7 and 8) and number of methyl substitutions (e.g., 0, 1 and 2) on the 6-membered ring were investigated. Copolymers with similar hydrophobic strengths (e.g., PC7A vs. PC6S1A; PC8A vs. PC6S2A) share similar pKa values despite different polymer architectures and CTL response (see **Fig. 1b**).
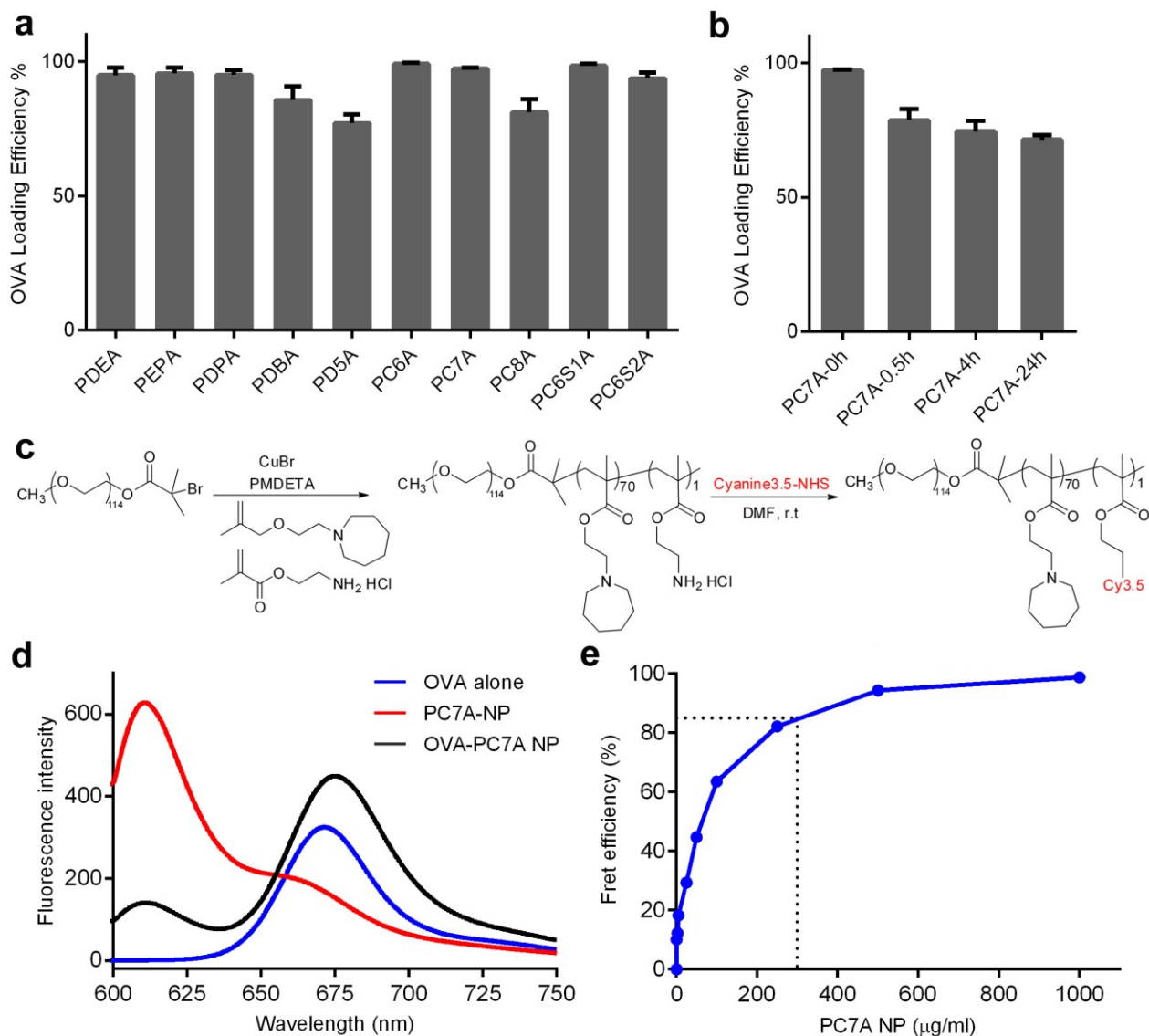
Supplementary Figure 2

Efficient loading of OVA in PC7A NP through a physical mixing procedure.

(**a**) The OVA loading efficiency in the micelle nanoparticles was measured by an ultrafiltration method. (**b**) Loading stability of OVA in PC7A micelles was examined in PBS buffer (pH 7.4) containing 5% fetal bovine serum at different time points. (**c**) Schematic synthesis of dye-conjugated PEG-*b*-PC7A copolymer. Cy3.5 was used as a dye example. (**d**) Fluorescence spectra of Cy3.5 labelled PC7A, AF647-OVA and PC7A+OVA mixture, which showed strong fluorescence resonance electron transfer (FRET) effect in the mixture group indicating OVA loading inside PC7A NP. (**e**) AF647-OVA (100μg/mL) was incubated with serially diluted Cy3.5-conjugated PC7A in PBS buffer (pH = 7.4), dotted line showed the working concentration of nanovaccine and its FRET efficiency. In **a** and **b**, representative data from three independent experiments are presented as means ± s.e.m..
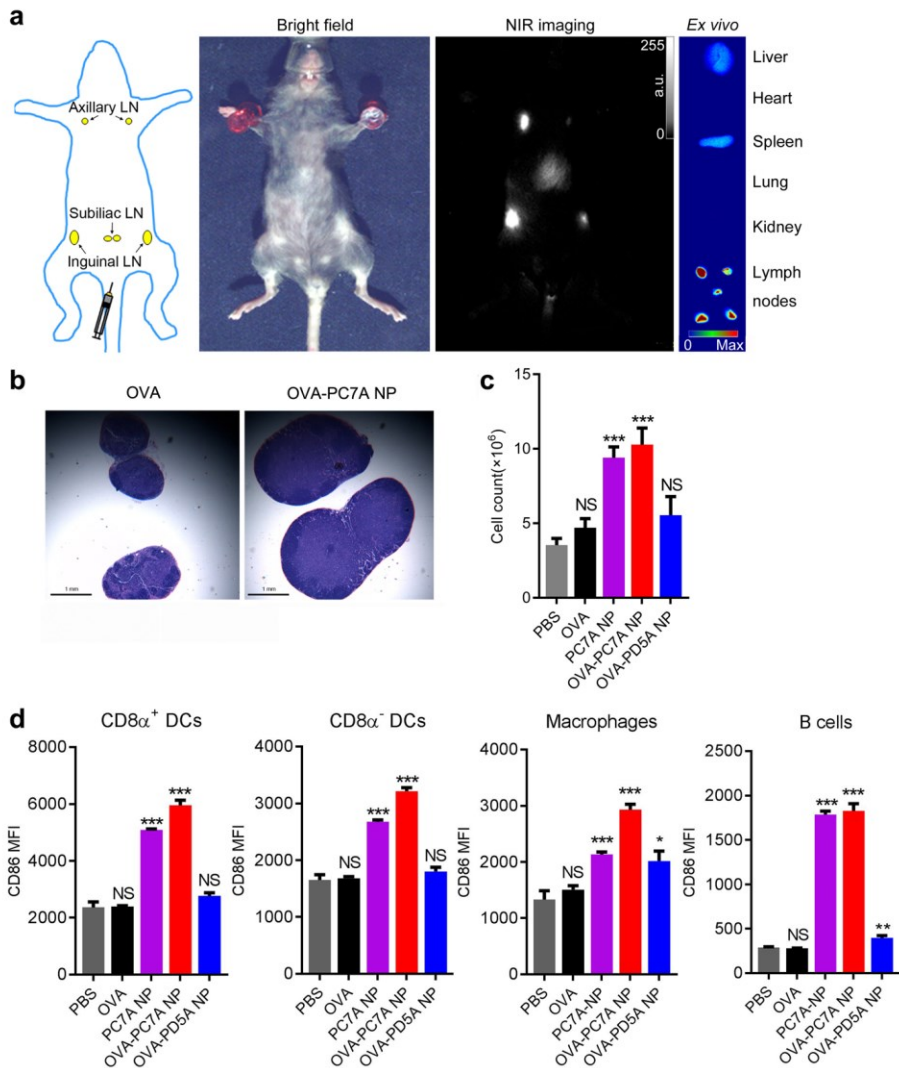
Supplementary Figure 3

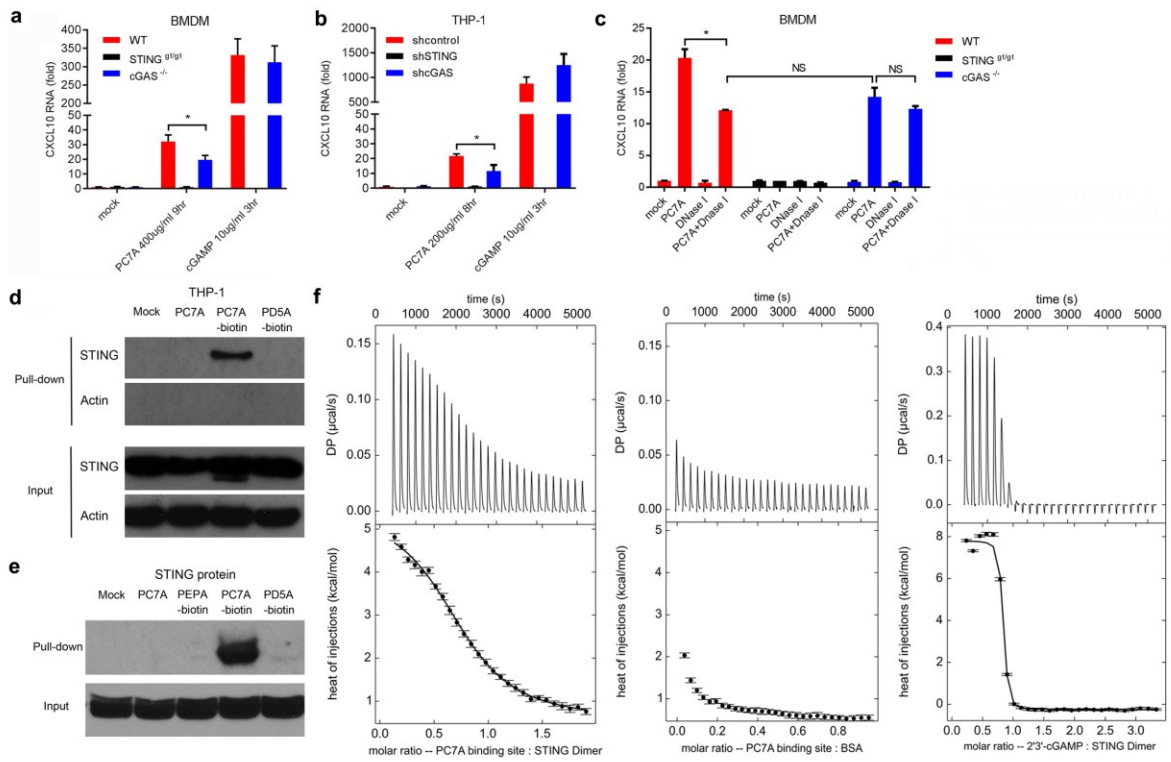**PC7A NP improves antigen delivery in draining lymph nodes, induces LN inflammation and APC maturation.**

(**a**) Near infrared imaging of ICG-labelled PC7A NP accumulation in lymphoid organs after subcutaneous injection at the tail base of C57BL/6 mice (n=3). After 24 h, lymph nodes and major organs were collected, and *ex vivo* imaging showed high PC7A NP accumulation in the lymph nodes over other organs. (**b**) Midline cross-section (maximal surface) of resected draining lymph nodes from C57BL/6 mice showed enlarged nodes by PC7A NP over OVA alone. (**c**) Quantification of total cell numbers in the draining lymph nodes at 24 h. Enlarged lymph nodes and increased cell number in the PC7A NP group indicate innate stimulation (n=5). (**d**) Quantitative comparison of CD86 expressions in CD8α$^+$, CD8α$^-$ DCs, macrophages and B cells in inguinal lymph nodes 24 h after injection of nanovaccine (n=5 for each group). In **c** and **d**, representative data from three independent experiments are presented as means ± s.e.m.. Statistical significance was calculated by Student's *t*-test, ***P<0.001, **P<0.01, *P<0.05. NS, not significant.
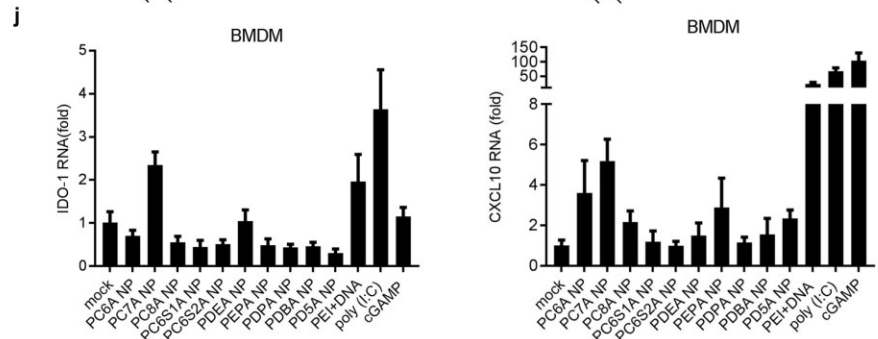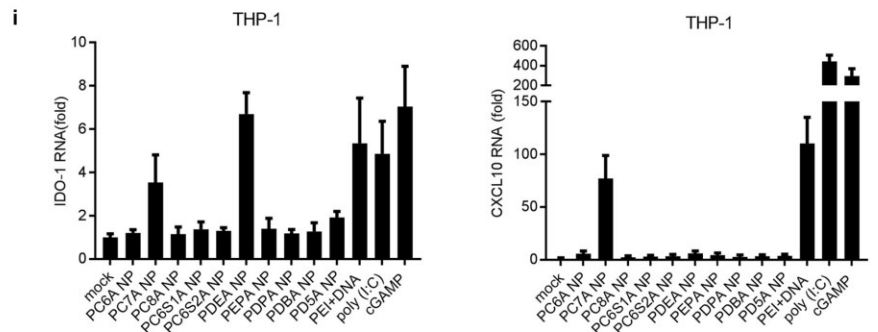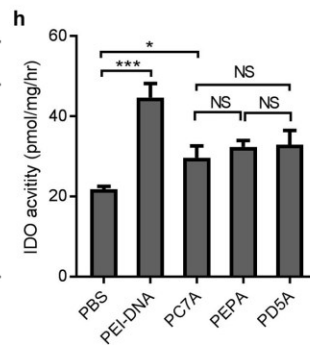
4
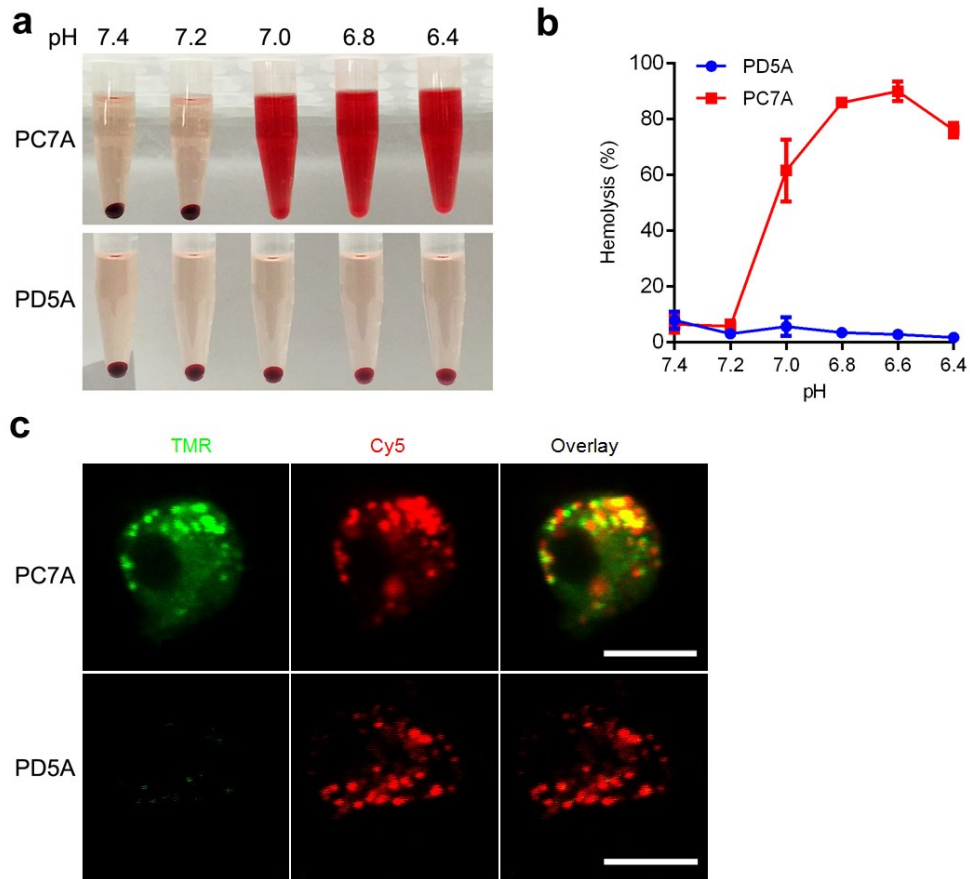
Supplementary Figure 4

PC7A NP disrupts membranes at acidic pH.

(**a**) Hemolytic analysis of the red blood cells after treatment with PC7A or PD5A copolymers in different pH medium. (**b**) Percentage of hemolysis was quantified by the release of hemoglobin into the medium as a function of pH for PC7A or PD5A NP (n=3). Both polymer concentrations were controlled at 20 μg/mL. (**c**) Confocal microscopy analysis of endo-lysosomal escape and cytosolic delivery of redox-activatable sensor-labeled OVA in live cells. DC2.4 cells were co-incubated with OVA (15 μg/mL) and PC7A or PD5A NP (50 μg/mL for copolymer concentration) for 30 min. Both the donor TMR (green) and acceptor Cy5 (red) signals from the redox-activatable sensor were imaged at 12 h after incubation. PC7A NP allowed higher amount of cytosolic delivery of OVA as indicated by the TMR donor signal. Scale bars = 10 μm. In **b,** representative data from three independent experiments are presented as means ± s.e.m..

a BMDM

CXCL10 RNA (fold) — WT (red), STING^gt/gt (black), cGAS^−/− (blue)
mock; PC7A 400ug/ml 9hr; cGAMP 10ug/ml 3hr

b THP-1

CXCL10 RNA (fold) — shcontrol (red), shSTING (black), shcGAS (blue)
mock; PC7A 200ug/ml 9hr; cGAMP 10ug/ml 3hr

c BMDM

CXCL10 RNA (fold) — WT (red), STING^gt/gt (black), cGAS^−/− (blue)
mock; PC7A; DNase I; PC7A+Dnase I

d THP-1

Pull-down: STING, Actin
Input: STING, Actin
Mock; PC7A; PC7A-biotin; PD5A-biotin

e STING protein

Pull-down
Input
Mock; PC7A; PEPA-biotin; PC7A-biotin; PD5A-biotin

f (ITC plots)
molar ratio -- PC7A binding site : STING Dimer
molar ratio -- PC7A binding site : BSA
molar ratio -- 2'3'-cGAMP : STING Dimer

g

	PC7A binding site : STING Dimer	PC7A : BSA	2'3'-cGAMP : STING Dimer
protein concentration (μM)	12.5	25	12.5
ligand concentration (μM)	110	110	180
K_d (nM)	1353	--	9.4
ΔH (kcal•mol^-1)	4.88	--	8.1
ΔS (cal•mol^-1K^-1)	43.5	--	64.2
ΔG (kcal•mol^-1)	- 7.87	--	- 10.76

h

IDO acvity (pmol/mg/hr)
PBS; PEI-DNA; PC7A; PEPA; PD5A

i THP-1

IDO-1 RNA(fold)
mock; PC6A NP; PC7A NP; PC8A NP; PC6S1A NP; PC6S2A NP; PDEA NP; PEPA NP; PDPA NP; PDBA NP; PD5A NP; PEI+DNA; poly (I:C); cGAMP

THP-1

CXCL10 RNA (fold)
mock; PC6A NP; PC7A NP; PC8A NP; PC6S1A NP; PC6S2A NP; PDEA NP; PEPA NP; PDPA NP; PDBA NP; PD5A NP; PEI+DNA; poly (I:C); cGAMP

j BMDM

IDO-1 RNA(fold)
mock; PC6A NP; PC7A NP; PC8A NP; PC6S1A NP; PC6S2A NP; PDEA NP; PEPA NP; PDPA NP; PDBA NP; PD5A NP; PEI+DNA; poly (I:C); cGAMP

BMDM

CXCL10 RNA (fold)
mock; PC6A NP; PC7A NP; PC8A NP; PC6S1A NP; PC6S2A NP; PDEA NP; PEPA NP; PDPA NP; PDBA NP; PD5A NP; PEI+DNA; poly (I:C); cGAMP

Supplementary Figure 5

PC7A NP activates type I IFN-induced genes through STING pathway.

Mouse bone marrow derived macrophages (BMDMs, **a**), human THP-1 monocytic cells (**b**) were incubated with PC7A NP at indicated concentration and time, followed by measurement of CXCL10 mRNA by qPCR (n=3). cGAMP, a STING activator transfected by lipofectamine was used as a positive control. Results show STING-dependent expression of CXCL10 in both cell lines. (**c**) BMDMs were transfected with DNase I for 1 hr, and followed by treatment with PC7A NP. CXCL10 mRNA was measured by qPCR (n=3). (**d**) PC7A NP treated THP-1 cells resulted in pulldown of STING proteins by streptavidin modified dynabeads. PD5A-biotin and PC7A only (biotin free) controls did not show any STING pulldown. (**e**) Direct pulldown assay of purified human STING C-terminal domain (CTD, 139-379AAs). PC7A-biotin copolymer pulled down STING CTD, but not other copolymers or PC7A only control. (**f**) Titration of PC7A binding to STING CTD by isothermal calorimetry (ITC) experiments. The original titration traces (top) and integrated data (bottom) were shown. ITC of PC7A-bovine serum albumin (BSA) was used as a negative control and cGAMP-STING CTD as a positive control. (**g**) Summary of binding affinity in ITC experiment. Negligible binding was found between PC7A and BSA. (**h**) Measurement of IDO enzyme activity in spleen cells after subcutaneous injection of different copolymers (150 μg, n=5). PEI-DNA (30 μg) was used as a positive control. (**i**) Human THP-1 and (**j**) mouse BMDM cells were treated with different NPs, followed by measurement of IDO-1 and CXCL10 mRNAs by qPCR (n=3). PEI-DNA, Poly(I:C) and cGAMP were used as positive controls. In **a-c,** and **i-j**, representative data from three independent experiments are presented as means ± s.e.m.. In **h**, representative data from two independent experiments are presented as means ± s.e.m.. Statistical significance was calculated by Student's *t*-test, ***P<0.001, **P<0.01, *P<0.05. NS, not significant.
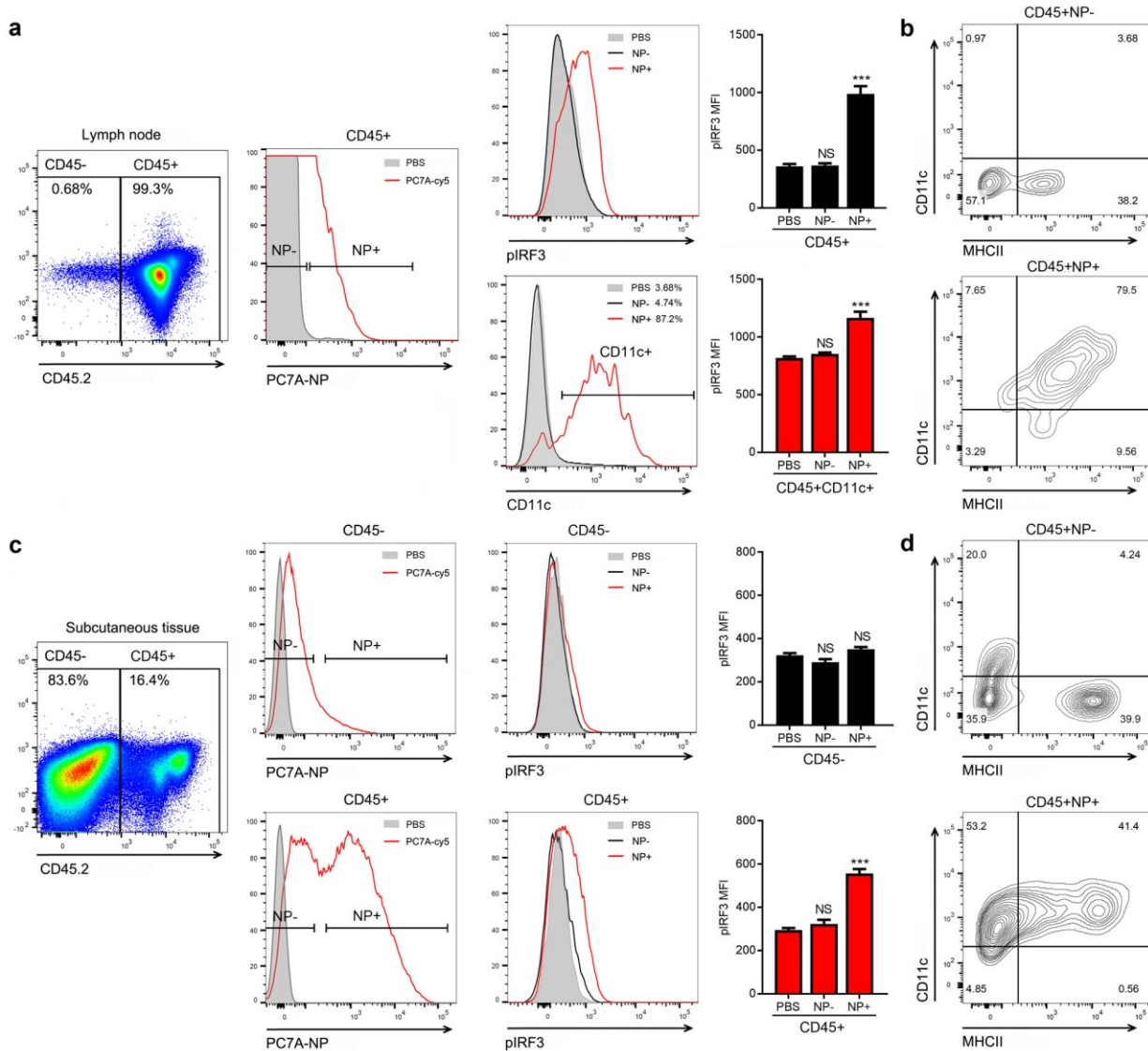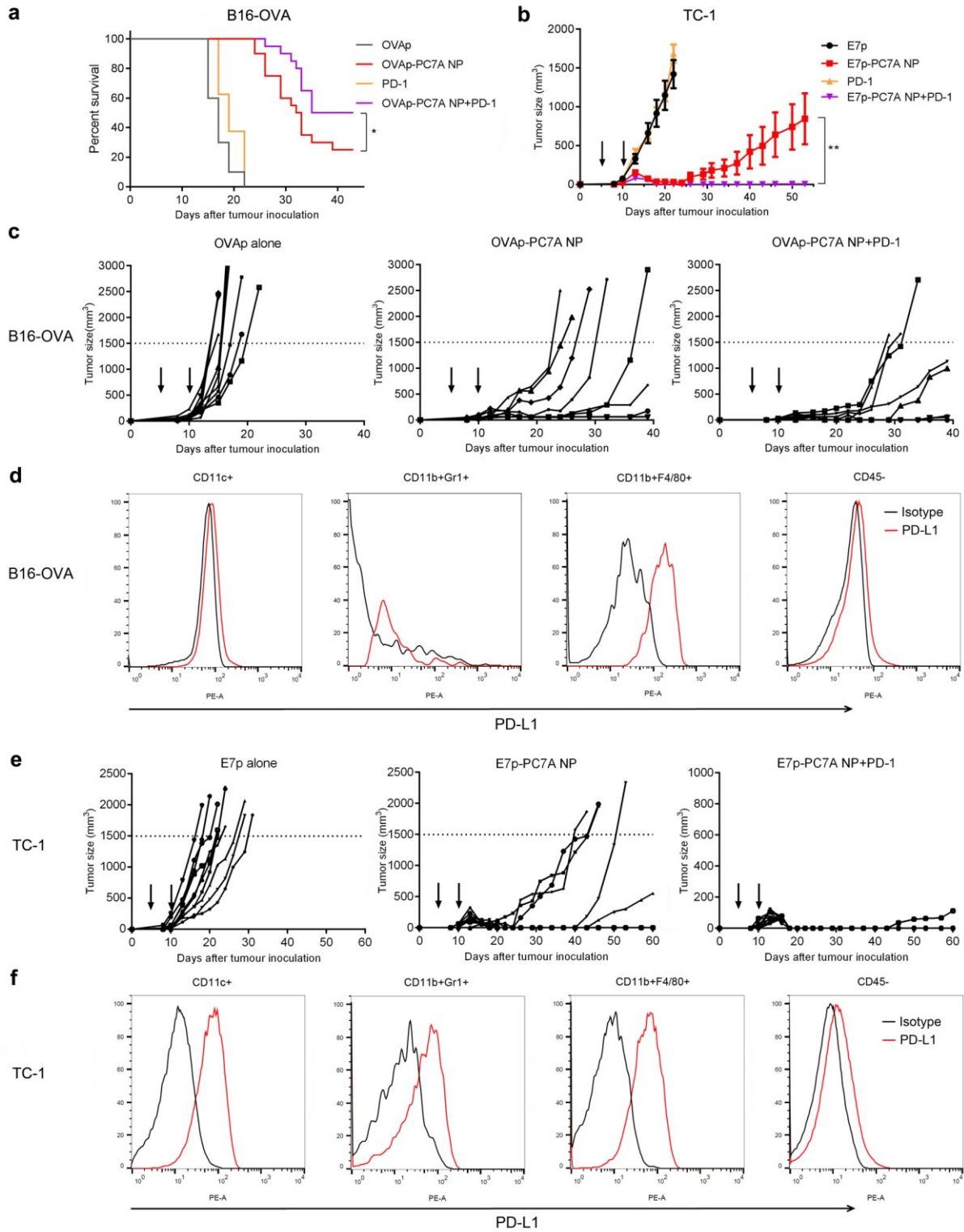
Supplementary Figure 6

APCs are the major cell population that take up PC7A NP and activate STING pathway *in vivo*.

PC7A NP-Cy5 was injected subcutaneously at the tail base of C57BL/6 mice, and PBS injected mice were included as control (n=5). After 24 hrs, inguinal LNs and subcutaneous tissue were isolated, and made into single cell suspension. Cells were first gated on live cells and then divided as leukocytes (CD45+) and non-leukocytes (CD45-). By the fluorescence of PC7A NP, cells from NP treated mice were divided into NP+ and NP- populations. The pIRF3 expression and DC marker CD11c were assessed in these subsets. (**a**) Comparative assessment of CD45+NP+ and CD45+NP- cells in LNs. (**b**) Phenotypic analysis of NP+ and NP- cells in LNs by flow cytometry. (**c**) Assessment of NP accumulated cells (NP+) in both CD45+ and CD45- cells from subcutaneous tissue. (**d**) Phenotypic analysis of CD45+NP- and CD45+ NP+ cells in subcutaneous tissue by flow cytometry.   In **a** and **c**, representative data from two independent experiments are presented as means ± s.e.m.. Statistical significance was calculated by Student's *t*-test, ***P<0.001. NS, not significant.

8
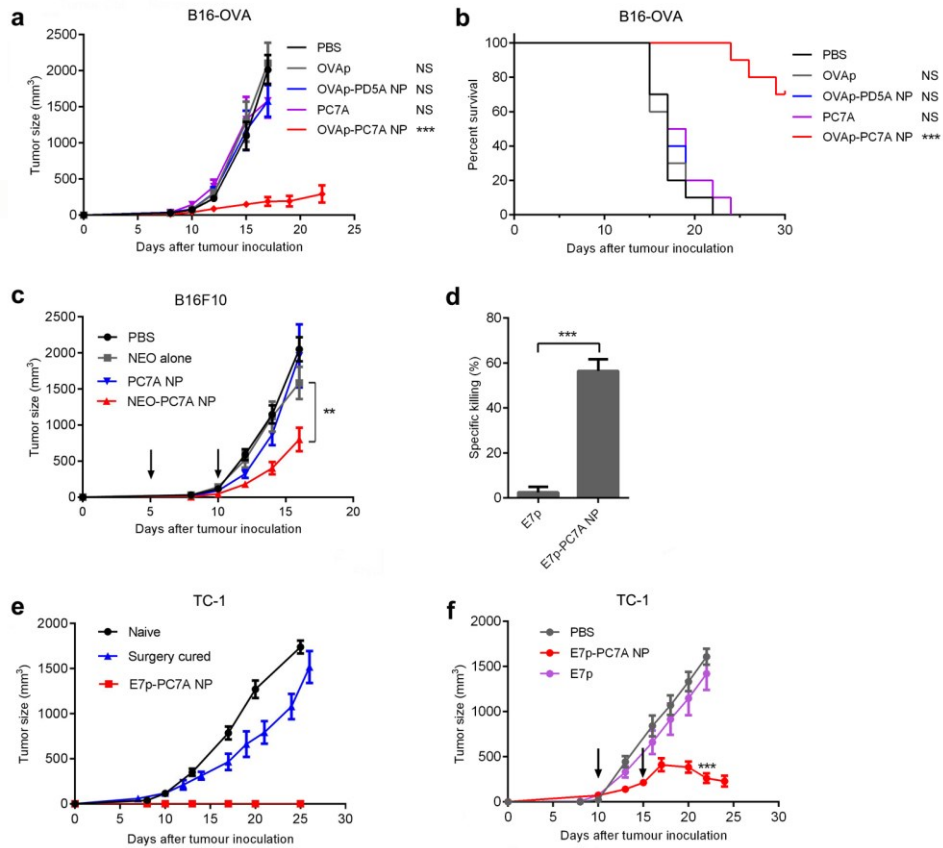
Supplementary Figure 7

PC7A nanovaccine inhibits tumor growth and prolongs survival. C57BL/6 mice (n=10 per group) were first inoculated with 1.5×10^5 B16-OVA tumor cells and followed by treatment with OVA peptide (0.5 µg), OVAp-PD5A NP, PC7A alone or OVAp-PC7A NP. PC7A NP alone without OVAp had no observable effect in tumor growth inhibition(**a**) or animal survival curves(**b**). (**c**) Tumor growth inhibition of B16F10 treated by neoantigen-PC7A NP. C57BL/6 mice (n=10 per group) inoculated with 1.5×10^5 B16F10 tumor cells were treated with a cocktail of neoantigens (Obsl1$_{T1764M}$, Kif18b$_{K739N}$, Def8$_{R255G}$) in PC7A NP (0.5 µg for each peptide, 30 µg polymer) per time points indicated by the arrows. (**d**) C57BL/6 mice (n=3 per group) were immunized with E7 peptide (E7p, 0.5 µg) and E7p-PC7A NP. E7-specific cytotoxicity was measured using an *in vivo* cytotoxicity killing assay. (**e**) Naïve mice or tumor-free mice 82 days after tumor inoculation in TC-1 model (n=10 per group) were challenged with 1×10^6 TC-1 tumor cells. On day 30 after surgery, mice were rechallenged with 1×10^6 TC-1 tumor cell. Memory T cells in the nanovaccine cured group completely inhibited tumor growth over 60 days. (**f**) Tumor growth inhibition curves in C57BL/6 mice (n=10 per group) inoculated with 1.5×10^5 TC-1 tumor cells and treated with nanovaccine at day 10 and 15 when tumors were established at ~100 mm^3. In **a** and **c-f**, data are presented as means ± s.e.m.. Statistical significance was calculated by Student's *t*-test, ***P<0.001, **P<0.01, *P<0.05. NS, not significant. Statistical significance for survival analysis in **b** was calculated by the log-rank test, ***P<0.001. NS, not significant.
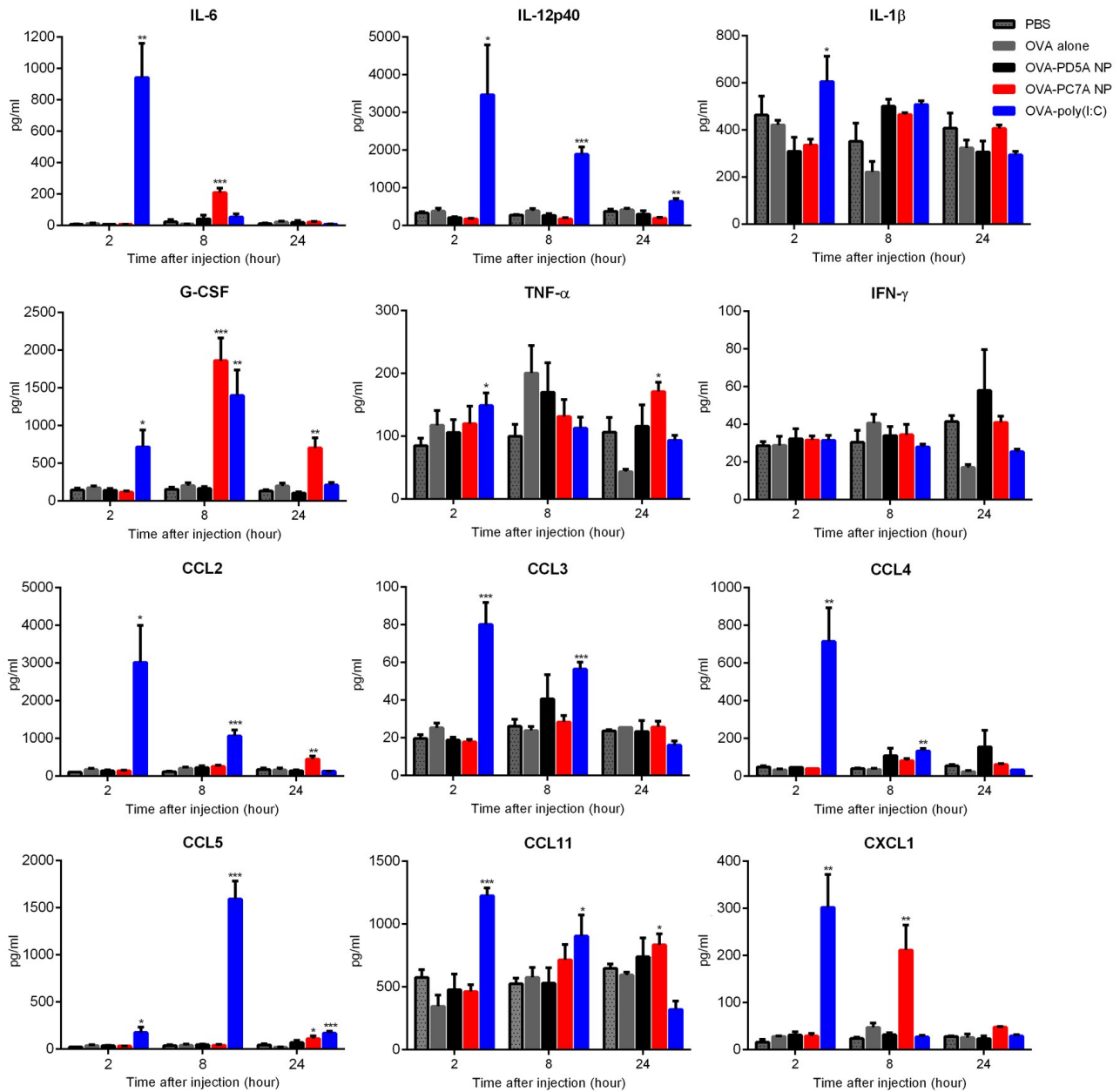
Supplementary Figure 8

Synergy effect of nanovaccine and anti-PD-1 antibody in two tumor models.

(**a**) C57BL/6 mice inoculated with 1.5×10^5 B16-OVA tumor cells were treated with OVA peptide, PC7A nanovaccine, anti-PD-1 alone and anti-PD-1 in combination with PC7A nanovaccine. Kaplan–

Meier survival curves of tumor-bearing mice were shown. (**b**) Long-term tumor growth inhibition curves in C57BL/6 mice (n=10 per group) inoculated with 1.5×10^5 TC-1 tumor cells followed by treatment with E7p (0.5 µg), PC7A nanovaccine, and a combination of anti-PD-1 and nanovaccine. (**c**) Individual tumor growth curves for OVAp alone, OVAp-PC7A NP, and OVAp-PC7A NP combined with anti-PD-1. (**d**) The PD-L1 expression profile in B16-OVA tumors. The PD-L1 were highly expressed in MDSCs (CD11b+Gr1+) and macrophages (CD11b+F4/80+) over the isotype control whereas the expression in DCs (CD11c+) and B16-OVA melanoma cells (CD45-) are modest. (**e**) Individual tumor growth curves for E7p alone, E7p-PC7A NP, and E7p-PC7A NP combined with anti-PD-1. Data show 50% and 90% of mice had tumor-free survival in the E7p-PC7A NP and E7p-PC7A NP/anti-PD-1 groups, respectively. (**f**) The PD-L1 expression profile in TC-1 tumors. The PD-L1 expressions were highly expressed in DCs, MDSCs, and macrophages over the isotype control whereas the expression in TC-1 tumor cells is modest. In **b**, data are presented as means ± s.e.m.. Statistical significance was calculated by Student's *t*-test, **P<0.01. Statistical significance for survival analysis in **a** was calculated by the log-rank test, *P<0.05.

Supplementary Figure 9

PC7A nanovaccine showed less systemic cytokine levels compared to Poly(I:C) control.
C57BL/6 mice (n=5 per group) were subcutaneously injected with 10 µg OVA plus 150 µg PC7A NP or the same dose of Poly(I:C). Systemic cytokines and chemokines in the serum were measured over time by bead-based Bio-Plex Pro Mouse Cytokine 23-plex Assay. IL-1α, IL-2, IL-3, IL-4, IL-5, IL-9, IL-10, IL-12 (p70), IL-13, IL-17, GM-CSF did not show any significant difference in all groups and were not included in this figure. Data are presented as means ± s.e.m.. Statistical significance was calculated by Student's t-test, ***P<0.001, **P<0.01, *P<0.05.
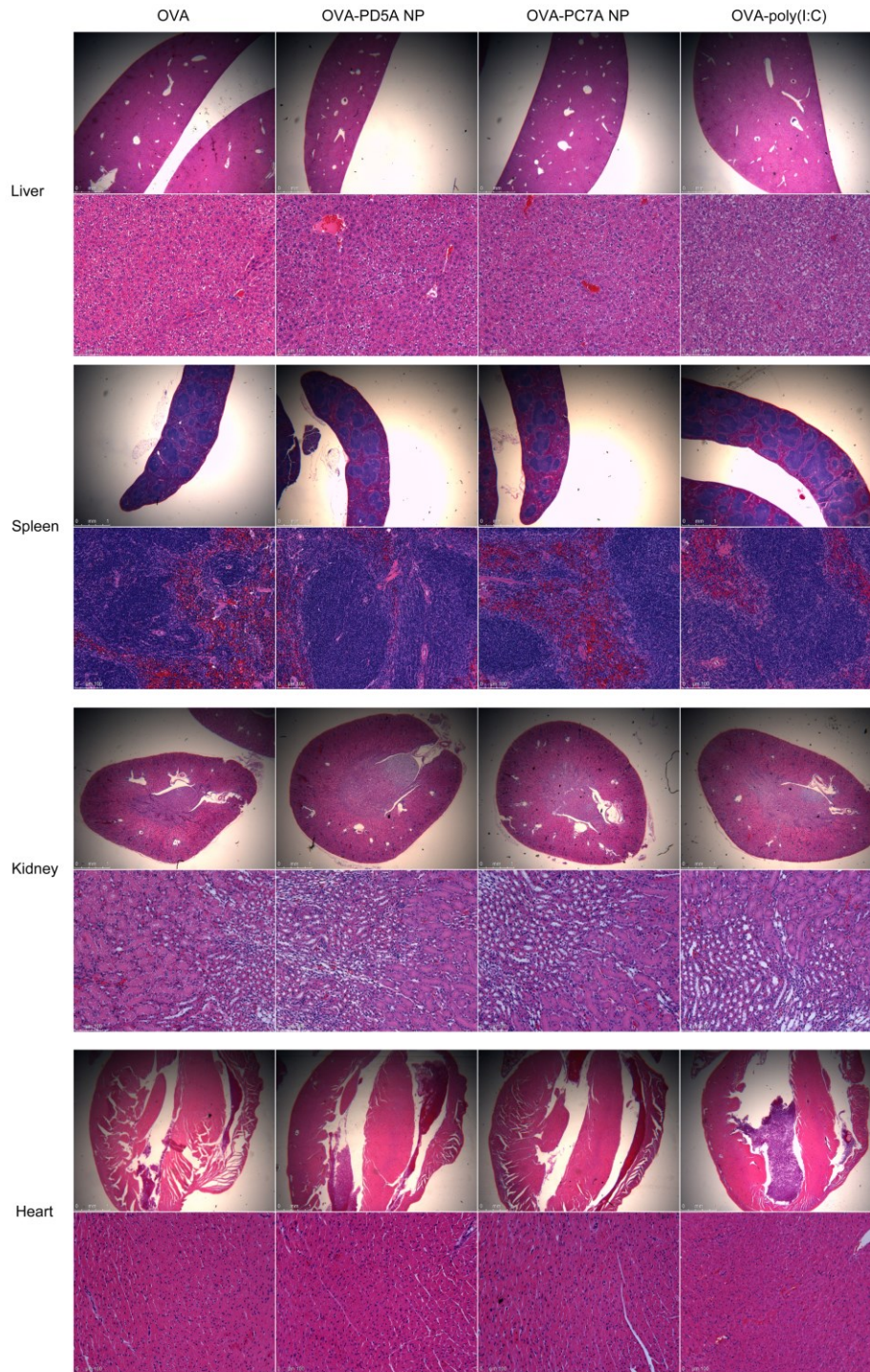
Supplementary Figure 10

Histology analyses of major organs for safety assessment of PC7A nanovaccine.

Representative H&E sections of the main organs from C57BL/6 mice after repeated injections of 10 μg OVA plus 150 μg PC7A NP or the same dose of Poly(I:C). Mice were sacrificed 24h after the second injection (n=5 for each group). Liver in Poly(I:C) group showed ballooned hepatocytes indicative of steatohepatitis. Spleen, kidney and heart showed no abnormalities for all the groups.